Original Article | Thoracic Imaging

http://dx.doi.org/10.3348/kjr.2015.16.5.1132
pISSN 1229-6929 · eISSN 2005-8330
Korean J Radiol 2015;16(5):1132-1141

Korean Journal of Radiology
KJR

Adaptive Statistical Iterative Reconstruction-Applied Ultra-Low-Dose CT with Radiography-Comparable Radiation Dose: Usefulness for Lung Nodule Detection

Hyun Jung Yoon, MD[1, 2], Myung Jin Chung, MD[1], Hye Sun Hwang, MD[1], Jung Won Moon, MD[3], Kyung Soo Lee, MD[1]

[1]Department of Radiology and Center for Imaging Science, Samsung Medical Center, Sungkyunkwan University School of Medicine, Seoul 06351, Korea; [2]Department of Radiology, Hanyang University Hospital, Hanyang University College of Medicine, Seoul 04763, Korea; [3]Department of Radiology, Kangbuk Samsung Hospital, Seoul 03181, Korea

Objective: To assess the performance of adaptive statistical iterative reconstruction (ASIR)-applied ultra-low-dose CT (ULDCT) in detecting small lung nodules.

Materials and Methods: Thirty patients underwent both ULDCT and standard dose CT (SCT). After determining the reference standard nodules, five observers, blinded to the reference standard reading results, independently evaluated SCT and both subsets of ASIR- and filtered back projection (FBP)-driven ULDCT images. Data assessed by observers were compared statistically.

Results: Converted effective doses in SCT and ULDCT were 2.81 ± 0.92 and 0.17 ± 0.02 mSv, respectively. A total of 114 lung nodules were detected on SCT as a standard reference. There was no statistically significant difference in sensitivity between ASIR-driven ULDCT and SCT for three out of the five observers (p = 0.678, 0.735, < 0.01, 0.038, and < 0.868 for observers 1, 2, 3, 4, and 5, respectively). The sensitivity of FBP-driven ULDCT was significantly lower than that of ASIR-driven ULDCT in three out of the five observers (p < 0.01 for three observers, and p = 0.064 and 0.146 for two observers). In jackknife alternative free-response receiver operating characteristic analysis, the mean values of figure-of-merit (FOM) for FBP, ASIR-driven ULDCT, and SCT were 0.682, 0.772, and 0.821, respectively, and there were no significant differences in FOM values between ASIR-driven ULDCT and SCT (p = 0.11), but the FOM value of FBP-driven ULDCT was significantly lower than that of ASIR-driven ULDCT and SCT (p = 0.01 and 0.00).

Conclusion: Adaptive statistical iterative reconstruction-driven ULDCT delivering a radiation dose of only 0.17 mSv offers acceptable sensitivity in nodule detection compared with SCT and has better performance than FBP-driven ULDCT.

Index terms: *Multidetector computed tomography; Image reconstruction; Adaptive statistical iterative reconstruction; Lung; Radiation dosage*

Received January 6, 2015; accepted after revision June 2, 2015.

Corresponding author: Myung Jin Chung, MD, Department of Radiology and Center for Imaging Science, Samsung Medical Center, Sungkyunkwan University School of Medicine, 81 Irwon-ro, Gangnam-gu, Seoul 06351, Korea.
• Tel: (822) 3410-6435 • Fax: (822) 3410-2559
• E-mail: mj1.chung@samsung.com

INTRODUCTION

Lung cancer is the most common cause of cancer death in both men and women in the industrialized world (1). Overall, 5-year survival for lung cancer (small cell lung cancer and non-small cell lung cancer) is 13% to 15%, and it has not shown any significant improvement over the last several decades (2). In contrast, when a stage I cancer is resected, the five-year survival rate is as high as 70% (3-6). Thus, detection of disease at an early stage is desirable.

Korean Journal of Radiology
KJR

Owing to advances in CT imaging techniques, screening for lung cancer has been suggested as a possible method for improving the patient outcome. It is widely used as a method for screening of lung metastases in patients with extra-thoracic malignancy where detection of metastases would influence treatment, as well as for detection of primary lung cancer. However, CT is associated with a relatively high level of ionizing radiation exposure and is not free from radiation risk. The radiation dose delivered during a chest CT study is in the range of 2–25 mSv, depending on the CT scanner and the examination protocol, and it is 10–1000 times greater than that delivered during chest radiography (7-11). In order to reduce radiation risk, low-dose CT techniques for lung cancer screening, which are generally defined as scanning techniques that use less than 100 mAs, are currently being implemented (12-15). Moreover, the latest article reported that the results of National Lung Screening Trial demonstrated that lung cancer screening with low-dose CT can provide 20% reduction in lung cancer mortality (16). Nevertheless, patient dose of low-dose CT is not low enough to provide complete protection from radiation risk (17, 18).

Dose reduction with CT has been limited because the current CT reconstruction algorithm (filtered back projection [FBP]) does not produce consistently diagnostic images if tube current is substantially reduced (19). Under the CT reconstruction algorithm of FBP, increased image noise is inherent in lowering the CT radiation dose (20). However, a new method for noise reduction based on iterative reconstruction algorithms, which enables one to correct image data using a system of models for image noise improvement, has recently been developed. Several studies have shown the benefit of iterative reconstruction for improving the image quality of chest CT (19-28). One of the first iterative reconstruction algorithms released for clinical use was the adaptive statistical iterative reconstruction (ASIR) algorithm. The ASIR algorithm significantly reduces image noise compared with the FBP algorithm, provides dose-reduced clinical images with preserved diagnostic value, and has been widely used for dose reduction in many CT systems (19-28).

However, to the best of our knowledge, these studies were not conducted with further reduced radiation dose for specific clinical applications and accuracy as endpoints. Therefore, the purpose of this study was to assess the performance of ASIR-applied ultra-low-dose CT (ULDCT) (< 0.2 mSv) in detecting small lung nodules in a clinical setting.

MATERIALS AND METHODS

Our Institutional Review Board approved this prospective study, and written informed consent was obtained from all study participants.

Patients

Thirty (mean age ± standard deviation, 60 ± 12 years; range, 29–78 years) consecutive patients (19 men [58 ± 13 years] and 11 women [62 ± 11 years]) underwent both ULDCT and standard dose CT (SCT). The weight of the patients ranged from 47.5 to 89 kg (mean weight, 64.5 kg). Main indications for CT studies were follow-up evaluation of lung nodules (n = 13), staging for lung malignancy (n = 8), or detection of metastatic pulmonary nodules in patients with an extra-thoracic malignancy (n = 9).

Image Acquisition and Reconstruction

Sixty-four-slice multi-detector CT (LightSpeed VCT XTe; GE Healthcare, Chalfont St. Giles, UK) was used for all chest CT examinations. Following ULDCT of the chest (individual detector width, 0.625 mm; tube voltage, 120 kVp; tube current, 10 mA; gantry rotation time, 0.5 seconds; pitch of 0.97) without contrast medium, all patients underwent a subsequent SCT (individual detector width, 0.625 mm; tube voltage, 120 kVp; tube current, 110–150 mA with automatic dose modulation; gantry rotation time, 0.5 seconds; pitch of 1.375) at suspended full inspiration after intravenous injection of contrast medium (iopromide, Ultravist 300; 80 mL, Bayer Healthcare, Berlin, Germany). ULDCT was considered as pre-contrast scan instead of standard dose pre-contrast scan (in our institute, we routinely perform a two-phase study using both pre-contrast and post-contrast scans). We fixed tube current at "10 mA" for ultra-low dose CT, because exposure to "10 mA" provides a similar radiation dose as that of radiography and Naidich et al. (29) demonstrated the potential of CT performed using "10 mA" tube current in their clinical study.

All 30 ULDCT examinations were reconstructed twice, once with the FBP technique and once with the ASIR (application of ASIR ratio, 60%) technique. The ASIR uses information obtained from the FBP algorithm as an initial building block for image reconstruction. The ASIR then uses matrix algebra to transform the measured value of each pixel to a new estimate of the pixel value. This pixel value is then compared with the ideal value that the noise model predicts. The process is repeated in successive iterative

steps until the final estimated and ideal pixel values ultimately converge. Using this method, ASIR is able to selectively identify and then subtract noise from an image. Thus, ASIR reconstructs images with lower image noise compared with FBP technique (23).

Adaptive statistical iterative reconstruction percentage can be selected in a spectrum of 0–100%, where 0% means all FBPs and 100% means all ASIRs. With the increase in the percentage, noise decreases. However, at higher levels of blending, contours of the structures begin to blur (19, 25, 27). The 60% level was chosen on the basis of our preliminary analysis, which indicated that 60%-ratio ASIR could produce a least noise image with diagnostically acceptable image quality. ASIR blending of more than 60% resulted in deteriorated image quality which readers could not accept. ASIR- and FBP-driven axial CT images were reconstructed with a 36–38 cm field of view, 2.5-mm-section thickness, and a high-spatial-frequency algorithm. All scan data were directly displayed on the picture archiving and communication system (PACS) (Centricity RA 1000; GE Healthcare) workstation monitors, and full functionality of the PACS software was available to the participating radiologists (e.g., window and level settings, zoom function etc.).

Ground-Truth Nodules at a Reference Standard Reading

Standard dose CT served as a reference standard for the determination of ground-truth lung nodules. SCT images were reviewed and assessed for the presence and characteristics of lung nodules by two subspecialty-trained chest radiologists (with 12 and 22 years of experience in chest CT interpretation, respectively). Decisions on the findings of lung nodule characteristics were reached by consensus. Nodule size was measured electronically on the PACS monitor. The size of the ground-truth lung nodules was determined as ≥ 3 mm in the long-axis diameter. Nodule characteristics for two categories (location and solidity) were assessed by the two radiologists, and then classified into two subgroups according to the location (peripheral for lung areas within 2 cm of the pleural surfaces and central for all remaining parenchyma) and into three subgroups based on solidity (ground-glass opacity, solid, and part-solid: ground-glass opacity with solid component). Subpleural or intrapulmonary lymph nodes were included in the reference standard as significant nodules. Calcified nodules were excluded from the reference standard.

Pulmonary Nodule Detection on ULDCT and SCT Images

Five other independent radiologists with four to ten years of experience in chest CT interpretation, who did not take part in the determination process for reference standard nodules with the use of SCT, assessed the three sets of images using the PACS system in a random order; namely, the ASIR-driven ULDCT, FBP-driven ULDCT, and SCT scans. Because the sensitivity for lung nodule detection on SCT scan for an observer was expected to be imperfect (rather somewhat lower than that in a reference standard reading), it was necessary that the same five observers reviewed the SCT scans.

The five observers, who were blinded to patient data and clinical information, were given the following instructions: to identify all non-calcified pulmonary nodules with long-axis diameters of 3 mm or greater with a caliper on the monitor using a procedure similar to that used in routine clinical practice; to report the location (central and peripheral) and solidity of each candidate nodule (ground-glass opacity, solid, and part-solid), and to assign a confidence level for each nodule using a 9-point scale ranging from 1 (nodule probably not present) to 9 (nodule definitely present), according to the free-response receiver operating characteristic (ROC) paradigm. During each session, the radiologists were given an unlimited amount of time to independently analyze the images.

Statistical Analysis

The results were used to generate the jackknife alternative free-response receiver operating characteristic (JAFROC) plots. The JAFROC analysis (30, 31) was used for the evaluation of observer performance in the detection of pulmonary nodules in the FBP-driven ULDCT, ASIR-driven ULDCT, and SCT. The JAFROC analysis has been proposed for estimating the statistical significance of differences between modalities when location issues are relevant and has been widely used in multiple previous studies in the radiology literature (32-35). The JAFROC analysis is based on a FROC paradigm and accounts for observer variation (30, 31). For statistical analysis of differences in observer performance among the FBP-driven ULDCT, ASIR-driven ULDCT, and SCT, JAFROC version 4.0 software was applied to estimate the figure-of-merit (FOM) values (analog of the area under the ROC curve, defined as the probability that a true-positive confidence rating exceeds any false-positive rating on cases without nodules) for each modality (the FBP-driven ULDCT, ASIR-driven ULDCT, and SCT) with 95%

Korean Journal of Radiology
KJR

confidence intervals. An F test was used internally for the analysis of variance, yielding a *p* value for rejecting the null hypothesis of no difference among the 3 modalities. A *p* value < 0.05 was considered statistically significant.

For the evaluation of diagnostic performance of ULDCT (ASIR-driven and FBP-driven images) and SCT scans read by five independent observers in detecting pulmonary nodules, the sensitivity of three different readings was calculated. Additionally, for each observer, we attempted to determine whether there was any significant difference in sensitivity for detecting lung nodules between ASIR-driven ULDCT and SCT images, and between FBP-driven ULDCT and SCT images. In all five observers, a similar analysis was performed among the three subgroups related to their size, shape, and location.

A Cochran's Q test was used for multiple statistical comparisons of the three CT protocols (FBP-driven ULDCT, ASIR-driven ULDCT images, and SCT images). For the Cochran's Q test, *p* values < 0.05 were required for rejecting the null hypothesis. McNemar test was used as a post-hoc test for the comparison of sensitivity in each pair (ASIR-driven ULDCT vs. FBP-driven ULDCT, ASIR-driven ULDCT vs. SCT, and FBP-driven ULDCT vs. SCT). The number of false positives was counted per patient level and the absolute number of false positives was compared by using Friedman test and Wilcoxon signed rank test. The number of nodules classified into each category of nodule characteristics, namely location and solidity, was also compared with that on a reference standard reading. Statistical analyses were conducted by using a commercially available software program (SPSS, version 18.0; SPSS Inc., Chicago, IL, USA).

RESULTS

Radiation Dose

Mean $CTDI_{vol}$ with SCT and ULDCT was 5.30 ± 1.65 and 0.34 ± 0.01 mGy, respectively, converted effective doses in SCT and ULDCT were 2.81 ± 0.92 and 0.17 ± 0.02 mSv, respectively, and dose-length product of SCT and ULDCT was 200.99 ± 65.77 and 12.27 ± 1.17 mGy·cm (36), respectively. Mean effective diameter was 27.49 ± 1.84 cm, and size-specific dose estimates in SCT and ULDCT were 7.25 ± 2.11 and 0.47 ± 0.04 mGy, respectively (37). For calculating the effective diameter, anteroposterior, and lateral measurements were made on chest CT scan at the level of superior portion of the breast; these measurements typically corresponded to the largest slice in their respective scan regions.

Nodule Detection

Examples of small pulmonary nodules visualized on SCT and ULDCT scans (with both FBP- and ASIR-applied methods) are shown in Figures 1 and 2.

In 30 patients, 114 nodules were detected by a reference standard reading. On FBP-driven ULDCT images, observers 1, 2, 3, 4, and 5 detected 71, 66, 67, 55, and 61 nodules, respectively. On ASIR-driven images, observers 1, 2, 3, 4, and 5 detected 91, 86, 86, 64, and 67 nodules, respectively. On SCT images, observers 1, 2, 3, 4, and 5 detected 94, 89, 107, 76, and 79 true nodules, respectively (Table 1). The Cochran's Q test showed a significant difference in nodule detectability among the three CT protocols in all observers. The sensitivity of FBP-driven ULDCT was significantly lower than that of SCT in all observers; however, the difference in sensitivity between ASIR-driven ULDCT and SCT was not statistically significant in three out of the five observers (Table 2). The sensitivity of FBP-driven ULDCT was significantly lower than that of ASIR-driven ULDCT in three observers, and there was no statistically significant difference for the other two observers.

Observers 1, 2, 3, 4, and 5 detected 61, 35, 11, 22, and 75 false positive nodules on FBP-driven images and 70, 37, 9, 10, and 82 false positive nodules on ASIR-driven images, respectively. On SCT images, 84, 64, 16, 27, and 81 false positive nodules were detected by observers 1, 2, 3, 4, and 5, respectively (Table 3).

Nodule Characteristics

Nodule size ranged from 3.0 to 11.5 mm (mean size, 4.15 mm) in a reference standard reading with the use of SCT scans. Nodule characteristics in terms of their location and solidity on SCT and ULDCT images for each observer are presented in Table 1. Basically, for significantly large (≥ 3 mm) and non-calcified nodules (ground-truth lung nodules), sensitivity of ASIR-driven images was superior to that of FBP-driven images. ASIR-driven ULDCT images were more useful for the detection of peripherally located nodules and nodules with ground-glass opacity than FBP-driven images. As for centrally located nodules, the nodule detection rates on ASIR- and FBP-driven ULDCT images were variable among observers.

With respect to the results of ground-truth lung nodule detection, the sensitivity of FBP-driven ULDCT was significantly lower than that of SCT; however, the differences in sensitivity between ASIR-driven ULDCT and SCT were not statistically significant in three observers.

For the detection of nodules with ground-glass opacity including part-solid nodules, the sensitivity of FBP-driven ULDCT was significantly lower than that of SCT in four observers, whereas the differences in sensitivity between ASIR-driven ULDCT and SCT were not statistically significant in four observers (Table 2).

Jackknife Alternative Free-Response Receiver Operating Characteristic Analysis

Figure-of-merit values in the detection of all pulmonary nodules for 5 observers are summarized in Table 4. The results of JAFROC FOM Dorfman-Berbaum-Metz-multi-reader multi-case significance test are presented in Table 5. In the overall nodules, no significant difference was identified in the FOM values between ASIR-driven ULDCT and SCT (p =

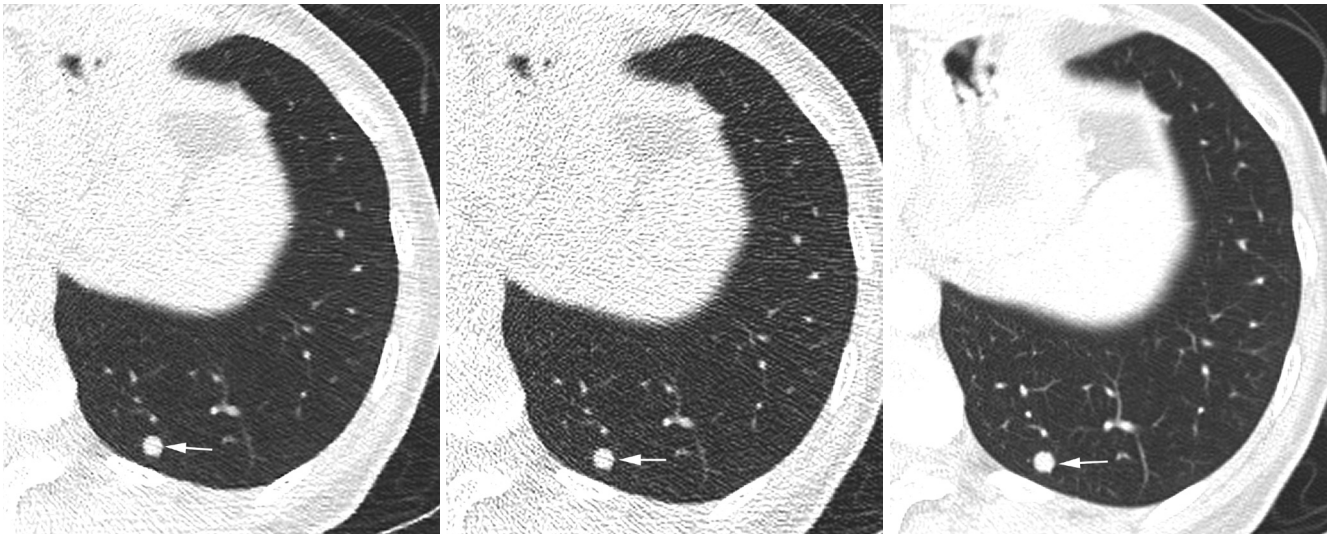

A B C

Fig. 1. Images of 43-year-old woman with metastatic lung nodule from rectal cancer show round pulmonary nodule measuring 5 mm (arrows) in left basal lung.

ASIR-driven ultra-low-dose CT **(A)**, FBP-driven ultra-low-dose CT **(B)**, and standard dose CT **(C)** images. All observers detected nodule on ASIR- and FBP-driven ultra-low-dose CT and on standard dose CT. Using ultra-low-dose CT, ASIR provides more acceptable image noise, better diagnostic acceptability, and visual sharpness of pulmonary nodule than FBP. ASIR = adaptive statistical iterative reconstruction, FBP = filtered back projection

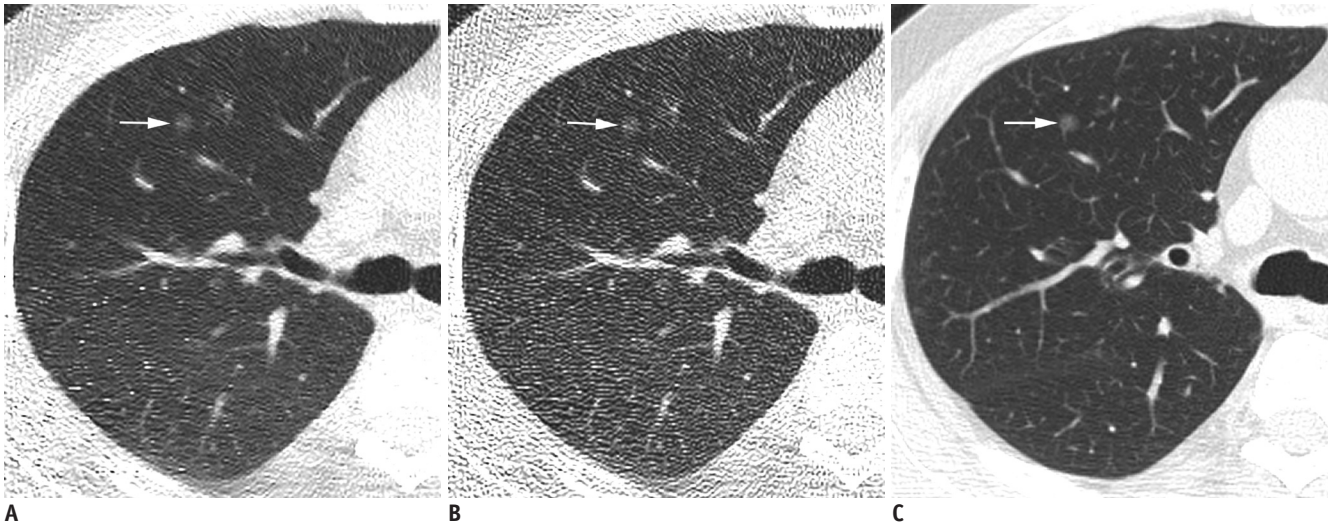

A B C

Fig. 2. Images of 45-year-old man with incidental pulmonary nodule show nodule with ground-glass opacity measuring 6 mm (arrows) in diameter in right upper lobe.

ASIR-driven ultra-low-dose CT **(A)**, FBP-driven ultra-low-dose CT **(B)**, and standard dose CT **(C)** images. Two observers could not detect nodule on ultra-low-dose CT scans with FBP reconstruction; however, all observers detected nodule on ASIR-driven ultra-low-dose CT scan and standard dose CT scan. ASIR = adaptive statistical iterative reconstruction, FBP = filtered back projection

Korean Journal of Radiology
KJR

0.11). However, there were significant differences between FBP-driven ULDCT and SCT, and between ASIR-driven ULDCT and FBP-driven ULDCT (p = 0.01 and 0.00).

DISCUSSION

Our results showed acceptable sensitivity for nodule detection on ASIR-driven ULDCT images as compared with

Table 1. Pulmonary Nodule Detection by Five Observers on ASIR- and FBP-Driven ULDCT Scans and on SCT Images

Number of Nodules	Total (n = 114)	Peripherally-Located Nodules (n = 87)	GGO Including PS (n = 33)
Observer 1			
FBP	71 (62)	53 (61)	17 (52)
ASIR	91 (80)	72 (83)	26 (79)
SCT	94 (82)	73 (84)	26 (79)
Observer 2			
FBP	66 (58)	53 (61)	16 (48)
ASIR	86 (75)	70 (80)	25 (76)
SCT	89 (78)	70 (80)	27 (82)
Observer 3			
FBP	67 (59)	53 (61)	19 (58)
ASIR	86 (75)	68 (78)	23 (70)
SCT	107 (94)	83 (95)	31 (94)
Observer 4			
FBP	55 (48)	41 (47)	13 (39)
ASIR	64 (56)	48 (55)	16 (48)
SCT	76 (67)	59 (68)	20 (61)
Observer 5			
FBP	61 (54)	46 (53)	13 (39)
ASIR	67 (59)	53 (61)	16 (48)
SCT	79 (61)	51 (59)	12 (36)

Numbers in parenthesis are percentage. ASIR = adaptive statistical iterative reconstruction, FBP = filtered back projection, GGO = ground-glass opacity, PS = part-solid, SCT = standard-dose CT, ULDCT = ultra-low-dose CT

Table 2. Results of Statistical Significances of Pulmonary Nodule Detectability by Five Observers in Terms of Various Nodule Characteristics

	Cochran's Q Test	Post-hoc (McNemar Test)		
		FBP vs. ASIR	FBP vs. SCT	ASIR vs. SCT
Total (n = 114)				
Observer 1	< 0.01*	< 0.01	< 0.01	0.678
Observer 2	< 0.01*	< 0.01	< 0.01	0.735
Observer 3	< 0.01*	< 0.01	< 0.01	< 0.01
Observer 4	< 0.01*	0.064	< 0.01	0.038
Observer 5	0.290	0.146	0.243	0.868
Peripherally-located nodules (n = 87)				
Observer 1	< 0.01*	< 0.01	< 0.01	< 0.01
Observer 2	< 0.01*	< 0.01	< 0.01	> 0.99
Observer 3	< 0.01*	< 0.01	< 0.01	< 0.01
Observer 4	< 0.01*	0.143	< 0.01	0.027
Observer 5	0.284	0.039	0.441	0.845
Ground glass nodules including part solid nodule (n = 33)				
Observer 1	< 0.01*	0.022	< 0.01	> 0.99
Observer 2	< 0.01*	< 0.01	0.019	0.774
Observer 3	< 0.01*	0.219	< 0.01	0.021
Observer 4	0.035*	0.375	0.039	0.289
Observer 5	0.236	0.250	> 0.99	0.289

*Values are significant by using Cochran's Q test (p < 0.05). ASIR = adaptive statistical iterative reconstruction, FBP = filtered back projection, SCT = standard-dose CT

Table 3. False Positive Pulmonary Nodule Detection by Five Observers on ASIR- and FBP-Driven ULDCT Scans and on SCT Images

	False Positive Nodules			Friedman Test	Wilcoxon Signed Rank Test		
	FBP	ASIR	SCT		FBP vs. ASIR	ASIR vs. SCT	SCT vs. FBP
Observer 1	61	70	84	0.648	0.376	0.363	0.215
Observer 2	35	37	64	0.034*	0.510	0.027	0.015
Observer 3	11	9	16	0.142	0.521	0.135	0.159
Observer 4	22	10	27	0.014*	0.030	0.012	0.260
Observer 5	75	82	81	0.659	0.431	0.456	0.867

*Values are significant by using Friedman test ($p < 0.05$). ASIR = adaptive statistical iterative reconstruction, FBP = filtered back projection, SCT = standard-dose CT, ULDCT = ultra-low-dose CT

Table 4. Figure-of-Merit Values Obtained from JAFROC Analysis

Observer	Modality		
	FBP	ASIR	SCT
1	0.717	0.823	0.846
2	0.632	0.785	0.808
3	0.742	0.785	0.946
4	0.612	0.726	0.750
5	0.709	0.742	0.753
Average	0.682	0.772	0.821

ASIR = adaptive statistical iterative reconstruction, FBP = filtered back projection, JAFROC = jackknife alternative free-response receiver operating characteristic, SCT = standard-dose CT

Table 5. Results of JAFROC FOM DBM-MRMC Significance Test

	Difference	*P*	95% CI	
			Low	High
SCT-FBP	0.090	0.01	0.028	0.152
ASIR-FBP	0.138	0.00	0.076	0.200
SCT-ASIR	0.048	0.11	-0.014	0.111

ASIR = adaptive statistical iterative reconstruction, CI = confidence interval, DBM-MRMC = Dorfman-Berbaum-Metz-multi-reader multi-case, FBP = filtered back projection, FOM = figure-of-merit, JAFROC = jackknife alternative free-response receiver operating characteristic, SCT = standard-dose CT

that in a reference standard reading and better performance of ASIR-driven ULDCT images than FBP-driven ULDCT images. There was no statistically significant difference in the observer sensitivity of pulmonary nodule detection between SCT and ASIR-driven ULDCT for three out of the five observers. The JAFROC analysis also revealed no significant differences between the ASIR-driven ULDCT and SCT. In the current study, by applying the ASIR technique, we used a significantly lower radiation dose of 0.17 mSv, which was two times less than the dose delivered during chest radiography (including posteroanterior and lateral projections). However, the data in this study showed that the detection rate of ASIR-driven ULDCT could not reach that of SCT. This result was inevitable because even conventional LDCT could not achieve the same diagnostic performance as SCT, particularly for detecting pulmonary nodules (15). Although this study has a limitation that we could not prove that the diagnostic performance of ASIR-driven ULDCT was equivalent to that of conventional FBP-driven LDCT, there was a significant improvement in its diagnostic performance compared with that of FBP-driven ULDCT and this was the primary goal of our study. If ASIR-driven ULDCT could show diagnostic performance equivalent to that of conventional LDCT in the next study, we can suggest its clinical usefulness for the establishment of minimum acceptable scanning parameters for lung cancer screening CT.

Several studies have shown the benefit of iterative reconstruction for improving the image quality of chest CT (19-26), with reported radiation dose levels of 1.8 mSv using iterative reconstruction in image space (21), 8.5–8.8 mSv using ASIR (23, 24), and 0.5–0.7 mSv using sinogram-affirmed iterative reconstruction (27). However, none of these studies have investigated the extremely-low-dose (less than 0.2 mSv) acquisition with clinical diagnosis. Also, model-based iterative reconstruction (MBIR) has been developed recently, which is a much more complex and advanced algorithm than ASIR and it has the potential to allow for further reductions in radiation dose without compromising image quality (38, 39). However, the MBIR technique is 20–30 times more time-consuming than the ASIR technique (27); therefore, it has a severe limitation in routine practice. Hence, thus far, ASIR has been considered as a useful technique in clinical practice.

Our study showed better results for SCT evaluation by two reference standard radiologists compared to the blinded reads by five ULDCT radiologists. There are several explanations for this phenomenon. Of course, these five readers were less experienced radiologists than the two reference standard radiologists, and that could have affected the results. However, the more important reason is that the sensitivity for independent reading in each image set was calculated only once without consensus.

Korean Journal of Radiology
KJR

The radiologists can feel exhausted because careful work and intense concentration are needed for performing these techniques, and single reading without consensus can lead to results showing less sensitivity. On the other hand, the data set on SCT evaluation made by two reference standard radiologists was established by double reading including a consensus report by the two radiologists (40-42). Therefore, a difference in results in terms of performance was observed between the two reference standard radiologists and five observers. Although there were differences in sensitivity among individual observers, the fundamental result, which suggested that ASIR-driven images had acceptable sensitivity in nodule detection than FBP-driven images, was consistent among observers.

In this study, there was a very large variability in false-positive nodule detection on SCT (up to 84 false positive nodules for one observer and as few as 16 false positive nodules for another observer). We speculate that variability related to observer inexperience as well as different personal attributes in CT reading (one is more sensitive, the other is more specific) probably caused a large variability in false-positive nodule detection on SCT as well as on ASIR and FBP-driven images.

Our scan protocol may be useful in detecting peripheral lung nodules. However in our study, ULDCT images were basically non-contrast-enhanced; thus may have led to poor performance in detecting central lung nodules. One study compared the sensitivity for pulmonary nodule detection between unenhanced conventional (200 mAs) and low dose (20 mAs) images (14), and the authors found that low-dose images detected 74% (107 of 144) of peripheral nodules, but only 58% (84 of 144) of central nodules. Therefore, irrespective of the radiation dose used, peripheral lung nodules are more readily detected than central lung nodules (even in ULDCT). ASIR-driven ULDCT allowed us to detect 64% of nodules with ground-glass opacity including part-solid nodules. Although sensitivity of 64% for the detection of nodules with ground-glass opacity was relatively low as compared with that for the detection of peripheral nodules (71%), the sensitivity of ASIR-driven ULDCT was superior to that of FBP-driven ULDCT.

Although images acquired by using the ASIR-driven ULDCT technique were better than those obtained by employing the FBP-driven technique, calcification-mimicking artifacts, thus precluding calcified nodule detection, were noted on ASIR-driven ULDCT images (Fig. 3). Also, aggressive implementation of iterative reconstruction is known to produce smoothing artifacts that resemble ground glass nodules (19, 25, 27). Such artifacts were also seen in our study and this might cause confusion in nodule categorization (Fig. 1). We chose the 60% noise reduction level for application of ASIR, and this level is the maximum limit for applying the appropriate setting of the ASIR. This was probably the reason why smoothing artifacts occurred in our study. Therefore, a further study is needed to determine the optimized noise reduction level which ensures a balance between noise reduction and smoothing artifacts. No other artifact was identified, and significant image noise was not detected on ULDCT images.

Our study has several limitations. First, there is no gold

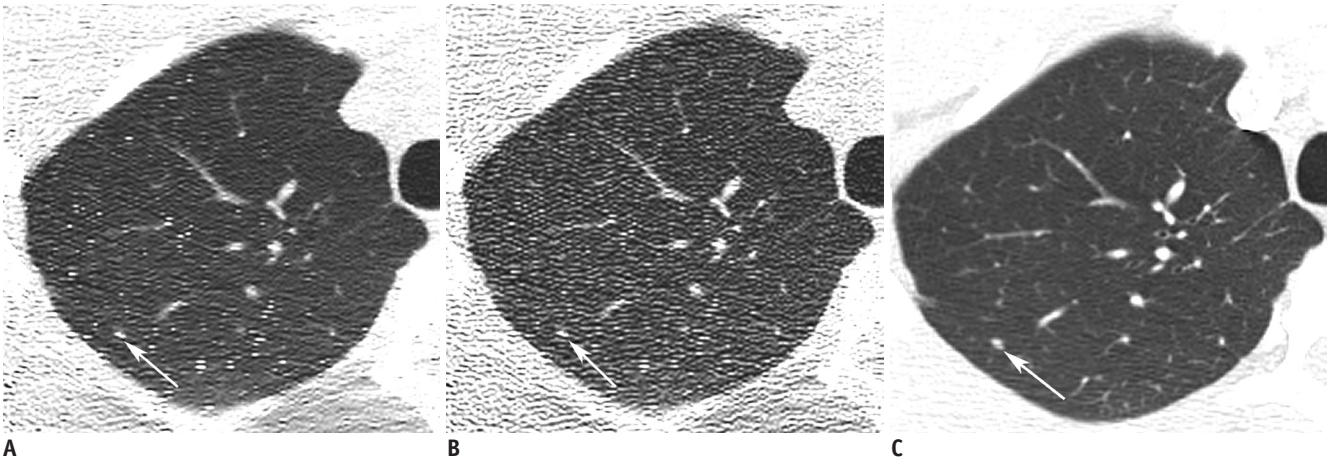

A B C

Fig. 3. Images of 29-year-old man with metastatic nodule from rectal cancer show nodule measuring 3 mm in diameter in right upper lobe.

A, B. Nodule was identified as calcified nodule by all observers on ASIR-driven ultra-low-dose CT **(A)** and FBP-driven ultra-low-dose CT **(B)** scans (arrow). **C.** This nodule was correctly read as metastatic nodule on standard dose CT scan (arrow). ASIR = adaptive statistical iterative reconstruction, FBP = filtered back projection

standard for the diagnosis of pulmonary nodules. Because we did not determine the pathological diagnosis of nodules in many patients, it is not exactly known how many lesions reported as nodules in a reference standard reading were true nodules (true positive), and how many of them were false nodules (false positive). Second, when the nodules seen both on SCT for reference standard reading and ULDCT for test reading were recorded, expert radiologists performed reference standard reading and observers performed test reading. Analysis by different groups may have cause a discrepancy between observers and reference standard reading. Finally, we did not apply variable conditions of tube current, variable blend ratios of ASIR technical mixing, and different reconstruction kernels for blended FBP technique. In addition, we did not assess the optimized tube voltage. These factors might have had an effect and could have resulted in different results in terms of image quality and lesion conspicuity. Further studies with different levels of the above-mentioned variables are necessary in order to compare lesion detection capabilities and to create the most suitable ULDCT protocol for lung nodule detection.

In conclusion, ASIR-applied ULDCT, with an effective radiation dose of approximately 0.17 mSv (comparable to the radiation dose of approximately 0.1 mSv for chest radiography), has an acceptable diagnostic performance compared with a reference standard reading for detecting clinically important small lung nodules by providing better and less noisy images than FBP reconstruction images with the same radiation dose. Based on our study, if a more suitable ASIR-applied ULDCT protocol can be created in future studies and it could show diagnostic performance of ASIR-applied ULDCT equivalent to that of conventional LDCT in the clinical field, the technique can be used in lung cancer screening and subsequent follow-up studies, particularly for the detection of peripherally located nodules or small nodules with ground-glass opacity, in which long-term follow-up evaluation is needed.

REFERENCES

1. Greenlee RT, Murray T, Bolden S, Wingo PA. Cancer statistics, 2000. *CA Cancer J Clin* 2000;50:7-33
2. Fry WA, Menck HR, Winchester DP. The National Cancer Data Base report on lung cancer. *Cancer* 1996;77:1947-1955
3. Flehinger BJ, Kimmel M, Melamed MR. The effect of surgical treatment on survival from early lung cancer. Implications for screening. *Chest* 1992;101:1013-1018
4. Melamed MR, Flehinger BJ, Zaman MB. Impact of early detection on the clinical course of lung cancer. *Surg Clin North Am* 1987;67:909-924
5. Nesbitt JC, Putnam JB Jr, Walsh GL, Roth JA, Mountain CF. Survival in early-stage non-small cell lung cancer. *Ann Thorac Surg* 1995;60:466-472
6. Shah R, Sabanathan S, Richardson J, Mearns AJ, Goulden C. Results of surgical treatment of stage I and II lung cancer. *J Cardiovasc Surg (Torino)* 1996;37:169-172
7. Evans SH, Davis R, Cooke J, Anderson W. A comparison of radiation doses to the breast in computed tomographic chest examinations for two scanning protocols. *Clin Radiol* 1989;40:45-46
8. Lenzen H, Roos N, Diederich S, Meier N. [Radiation exposure in low dose computerized tomography of the thorax]. *Radiologe* 1996;36:483-488
9. Parry RA, Glaze SA, Archer BR. The AAPM/RSNA physics tutorial for residents. Typical patient radiation doses in diagnostic radiology. *Radiographics* 1999;19:1289-1302
10. Van Unnik JG, Broerse JJ, Geleijns J, Jansen JT, Zoetelief J, Zweers D. Survey of CT techniques and absorbed dose in various Dutch hospitals. *Br J Radiol* 1997;70:367-371
11. Wall BF, Hart D. Revised radiation doses for typical X-ray examinations. Report on a recent review of doses to patients from medical X-ray examinations in the UK by NRPB. National Radiological Protection Board. *Br J Radiol* 1997;70:437-439
12. Gartenschläger M, Schweden F, Gast K, Westermeier T, Kauczor H, von Zitzewitz H, et al. Pulmonary nodules: detection with low-dose vs conventional-dose spiral CT. *Eur Radiol* 1998;8:609-614
13. Henschke CI, Yankelevitz DF, McCauley DI, Libby DM, Pasmantier MW, Smith JP. Guidelines for the use of spiral computed tomography in screening for lung cancer. *Eur Respir J Suppl* 2003;39:45s-51s
14. Rusinek H, Naidich DP, McGuinness G, Leitman BS, McCauley DI, Krinsky GA, et al. Pulmonary nodule detection: low-dose versus conventional CT. *Radiology* 1998;209:243-249
15. Diederich S, Lenzen H, Windmann R, Puskas Z, Yelbuz TM, Henneken S, et al. Pulmonary nodules: experimental and clinical studies at low-dose CT. *Radiology* 1999;213:289-298
16. National Lung Screening Trial Research Team, Aberle DR, Adams AM, Berg CD, Black WC, Clapp JD, et al. Reduced lung-cancer mortality with low-dose computed tomographic screening. *N Engl J Med* 2011;365:395-409
17. Brenner DJ, Elliston CD. Estimated radiation risks potentially associated with full-body CT screening. *Radiology* 2004;232:735-738
18. Brenner DJ, Hall EJ. Computed tomography--an increasing source of radiation exposure. *N Engl J Med* 2007;357:2277-2284
19. Hara AK, Paden RG, Silva AC, Kujak JL, Lawder HJ, Pavlicek W. Iterative reconstruction technique for reducing body radiation dose at CT: feasibility study. *AJR Am J Roentgenol* 2009;193:764-771
20. Kalra MK, Maher MM, Sahani DV, Blake MA, Hahn PF, Avinash GB, et al. Low-dose CT of the abdomen: evaluation of image

improvement with use of noise reduction filters pilot study. *Radiology* 2003;228:251-256
21. Pontana F, Duhamel A, Pagniez J, Flohr T, Faivre JB, Hachulla AL, et al. Chest computed tomography using iterative reconstruction vs filtered back projection (Part 2): image quality of low-dose CT examinations in 80 patients. *Eur Radiol* 2011;21:636-643
22. Pontana F, Pagniez J, Flohr T, Faivre JB, Duhamel A, Remy J, et al. Chest computed tomography using iterative reconstruction vs filtered back projection (Part 1): evaluation of image noise reduction in 32 patients. *Eur Radiol* 2011;21:627-635
23. Prakash P, Kalra MK, Digumarthy SR, Hsieh J, Pien H, Singh S, et al. Radiation dose reduction with chest computed tomography using adaptive statistical iterative reconstruction technique: initial experience. *J Comput Assist Tomogr* 2010;34:40-45
24. Prakash P, Kalra MK, Ackman JB, Digumarthy SR, Hsieh J, Do S, et al. Diffuse lung disease: CT of the chest with adaptive statistical iterative reconstruction technique. *Radiology* 2010;256:261-269
25. Yanagawa M, Honda O, Yoshida S, Kikuyama A, Inoue A, Sumikawa H, et al. Adaptive statistical iterative reconstruction technique for pulmonary CT: image quality of the cadaveric lung on standard- and reduced-dose CT. *Acad Radiol* 2010;17:1259-1266
26. Leipsic J, Nguyen G, Brown J, Sin D, Mayo JR. A prospective evaluation of dose reduction and image quality in chest CT using adaptive statistical iterative reconstruction. *AJR Am J Roentgenol* 2010;195:1095-1099
27. Willemink MJ, de Jong PA, Leiner T, de Heer LM, Nievelstein RA, Budde RP, et al. Iterative reconstruction techniques for computed tomography Part 1: technical principles. *Eur Radiol* 2013;23:1623-1631
28. Willemink MJ, Leiner T, de Jong PA, de Heer LM, Nievelstein RA, Schilham AM, et al. Iterative reconstruction techniques for computed tomography part 2: initial results in dose reduction and image quality. *Eur Radiol* 2013;23:1632-1642
29. Naidich DP, Marshall CH, Gribbin C, Arams RS, McCauley DI. Low-dose CT of the lungs: preliminary observations. *Radiology* 1990;175:729-731
30. Chakraborty DP, Berbaum KS. Observer studies involving detection and localization: modeling, analysis, and validation. *Med Phys* 2004;31:2313-2330
31. Chakraborty DP. Analysis of location specific observer performance data: validated extensions of the jackknife free-response (JAFROC) method. *Acad Radiol* 2006;13:1187-1193
32. Vikgren J, Zachrisson S, Svalkvist A, Johnsson AA, Boijsen M, Flinck A, et al. Comparison of chest tomosynthesis and chest radiography for detection of pulmonary nodules: human observer study of clinical cases. *Radiology* 2008;249:1034-1041
33. Hirose T, Nitta N, Shiraishi J, Nagatani Y, Takahashi M, Murata K. Evaluation of computer-aided diagnosis (CAD) software for the detection of lung nodules on multidetector row computed tomography (MDCT): JAFROC study for the improvement in radiologists' diagnostic accuracy. *Acad Radiol* 2008;15:1505-1512
34. Zachrisson S, Vikgren J, Svalkvist A, Johnsson AA, Boijsen M, Flinck A, et al. Effect of clinical experience of chest tomosynthesis on detection of pulmonary nodules. *Acta Radiol* 2009;50:884-891
35. Yanagawa M, Honda O, Yoshida S, Ono Y, Inoue A, Daimon T, et al. Commercially available computer-aided detection system for pulmonary nodules on thin-section images using 64 detectors-row CT: preliminary study of 48 cases. *Acad Radiol* 2009;16:924-933
36. Larke FJ, Kruger RL, Cagnon CH, Flynn MJ, McNitt-Gray MM, Wu X, et al. Estimated radiation dose associated with low-dose chest CT of average-size participants in the National Lung Screening Trial. *AJR Am J Roentgenol* 2011;197:1165-1169
37. Boone JM, Strauss KJ, Cody DD, McCollough CH, McNitt-Gray MF, Toth TL, et al. *Size-specific dose estimates (SSDE) in pediatric and adult body CT examinations. Report of AAPM Task Group 204*. College Park: American Association of Physicists in Medicine, 2011
38. Katsura M, Matsuda I, Akahane M, Yasaka K, Hanaoka S, Akai H, et al. Model-based iterative reconstruction technique for ultralow-dose chest CT: comparison of pulmonary nodule detectability with the adaptive statistical iterative reconstruction technique. *Invest Radiol* 2013;48:206-212
39. Neroladaki A, Botsikas D, Boudabbous S, Becker CD, Montet X. Computed tomography of the chest with model-based iterative reconstruction using a radiation exposure similar to chest X-ray examination: preliminary observations. *Eur Radiol* 2013;23:360-366
40. Wormanns D, Ludwig K, Beyer F, Heindel W, Diederich S. Detection of pulmonary nodules at multirow-detector CT: effectiveness of double reading to improve sensitivity at standard-dose and low-dose chest CT. *Eur Radiol* 2005;15:14-22
41. Seltzer SE, Judy PF, Adams DF, Jacobson FL, Stark P, Kikinis R, et al. Spiral CT of the chest: comparison of cine and film-based viewing. *Radiology* 1995;197:73-78
42. Diederich S, Semik M, Lentschig MG, Winter F, Scheld HH, Roos N, et al. Helical CT of pulmonary nodules in patients with extrathoracic malignancy: CT-surgical correlation. *AJR Am J Roentgenol* 1999;172:353-360